Arabian Journal of Chemistry (2014) 7, 732–740

King Saud University

Arabian Journal of Chemistry

www.ksu.edu.sa
www.sciencedirect.com

ORIGINAL ARTICLE

An experimental and theoretical investigation on adsorption properties of some diphenolic Schiff bases as corrosion inhibitors at acidic solution/mild steel interface

Aysel Yurt [a,*], **Berrin Duran** [a], **Hakan Dal** [b]

[a] *Eskişehir Osmangazi University, Faculty of Arts and Science, Department of Chemistry, 26480 Eskişehir, Turkey*
[b] *Anadolu University, Faculty of Science, Department of Chemistry, 26470 Eskişehir, Turkey*

Received 27 October 2010; accepted 3 December 2010
Available online 13 December 2010

KEYWORDS

Corrosion inhibitor;
Mild steel;
Schiff bases;
Chemisorption;
Polarization measurements;
EIS;
Quantum chemical calculations

Abstract The effect of novel synthesized three Schiff bases, namely, 1,3-bis[2-(2-hydroxy benzylidenamino) phenoxy] propane (P1), 1,3-bis[2-(5-chloro-2-hydroxybenzylidenamino) phenoxy] propane (P2), and 1,3-bis[2-(5-bromo-2-hydroxybenzylidenamino) phenoxy] propane (P3), on the corrosion of mild steel in 0.1 M HCl was investigated using potentiodynamic polarization and electrochemical impedance spectroscopy methods. Polarization measurements suggest that P1 acts as mixed type inhibitor while P2 and P3 behave as mainly cathodic inhibitors for acidic corrosion of steel. All electrochemical measurements show that inhibition efficiencies increase with increase in inhibitor concentration. This reveals that inhibitive actions of inhibitors were mainly due to adsorption on steel surface. Adsorption of these inhibitors follows Temkin adsorption isotherm. The correlation between the adsorption ability of inhibitors and their molecular structures has been investigated using quantum chemical parameters obtained by MNDO semi-empirical method. Calculated quantum chemical parameters indicate that Schiff bases adsorbed on steel surface by chemical mechanism.

1. Introduction

Steel is extensively used in various industrial operations and the study of its corrosion inhibition in pickling bath is of great importance. The use of inhibitors is one of the practical methods for protection against corrosion in especially acidic media (Nathan, 1977; Trabanelli, 1991; Bahrami et al., 2010; Fouda and Ellithy, 2009). Most of the effective inhibitors are organic compounds combining nitrogen, oxygen, phosphorous and sulphur in their structures (Clubby, 1990; Stupnisek-Lisac

---

[*] Corresponding author. Tel.: +90 222 2393750x2866; fax: +90 222 2393578.
E-mail address: ayurt@ogu.edu.tr (A. Yurt).

Peer review under responsibility of King Saud University.

Production and hosting by Elsevier

http://dx.doi.org/10.1016/j.arabjc.2010.12.010

and Ademovic, 1995; Özcan et al., 2004; Moretti et al., 1996). The inhibiting actions of organic compounds are usually attributed to their interactions with the metal surface via their adsorption. These compounds in general are adsorbed on the metal surface, blocking the active corrosion sites. Four types of adsorption may take place by organic molecules at metal/solution interface: (1) electrostatic attraction between the charged molecules and the charged metal, (2) interaction of unshared electron pairs in the molecule with the metal, (3) interaction of π electrons with the metal and (4) combination of (1) and (3) (Shokry et al., 1998).

The adsorption ability of inhibitors onto metal surface depends on the nature and surface charge of metal, the chemical composition of electrolytes, and the molecular structure and electronic characteristics of inhibitor molecules. Organic compounds containing functional electronegative groups and π-electrons in triple or conjugated double bonds are usually good inhibitors (Yurt et al., 2004; Ju et al., 2008; Ahamad et al., 2010a). Schiff bases, with RC=NR′ as general formula, have both the features combined with their structure which may then give rise to particularly potential inhibitors.

Schiff bases are condensation products of an amine and a ketone or aldehyde. The greatest advantage of Schiff bases is that they can be easily synthesized from relatively inexpensive materials. Some Schiff bases have been recently reported as effective corrosion inhibitors for steel, aluminium and copper in acidic media (Bain et al., 1989; Emregül et al., 2003; Gomma and Wahdan, 1995; Yurt et al., 2006; Li et al., 1999a,b; Negm and Zaki, 2008).

The purpose of the present study is to investigate the effect of 1,3-bis[2-(2-hydroxybenzylidenamino)phenoxy]propane, 1,3-bis[2-(5-chloro-2-hydroxybenzylidenamino) phenoxy]propane, and 1,3-bis[2-(5-bromo-2-hydroxybenzylidenamino)phenoxy]propane on the electrochemical behaviour of mild steel in 0.1 M HCl solution using electrochemical techniques. In order to investigate the relationship between inhibition efficiency and the structure of studied Schiff bases, some quantum chemical parameters such as HOMO and LUMO energies, charge density of adsorption centres, dihedral angles and dipole moment have also been calculated. Theoretical approaches provide means of analyzing metal-inhibitor interactions and there are many reports related with this area (Yurt et al., 2005a,b; Bentiss et al., 2002).

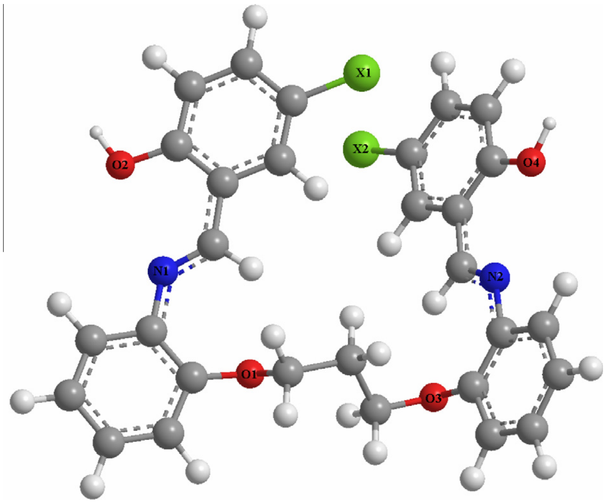

Figure 1 Molecular structure of investigated Schiff bases (P1; X = H, P2; X = Cl, P3; X = Br).

2. Experimental

2.1. Materials and sample preparation

The Schiff base compounds used were synthesized by condensation reaction between 1.9 mmol 1,3-bis(*o*-aminophenoxy)-3-oxopropane and the corresponding aldehydes (3.8 mmol) in 50 mL methanol and recrystallized in methanol-THF mixture. The aldehyde compounds used were salicylaldehyde, 5-chlorosalicylaldehyde and 5-bromosalicylaldehyde. All chemicals were purchased from Merck and were not purified further. The structures of all synthesized salicylaldimine Schiff bases, 1,3-bis[2-(2-hydroxybenzylidenamino) phenoxy] propane (P1), 1,3-bis[2-(5-chloro-2-hydroxybenzylidenamino)phenoxy]propane (P2), and 1,3-bis[2-(5-bromo-2-hydroxybenzylidenamino)phenoxy]propane (P3), were characterized by using elementary analyses, FT-IR, ^{13}C NMR and ^{1}H NMR spectroscopy techniques. The general structure of these inhibitors is given by Fig. 1.

2.2. Electrochemical experiments

Electrochemical experiments were performed using mild steel specimen with the following composition: 0.134% C, 0.0514% Ni, 0.555% Mn, 0.0117% P, 0.200% Si, 0.0258% S and balance Fe. A cylindrical steel rod (whose exposed surface area was 0.1963 cm^2) was inserted into a Teflon tube so that only the flat surface was in contact with test solution. Before each experiment, the electrode was polished with a sequence of emery papers of different grades (600, 800 and 1200), washed with double distilled water and degreased with acetone.

Electrochemical impedance (EIS) and potentiodynamic polarization (PP) studies were carried out using a Gamry PC3/600 potentiostat/galvanostat/ZRA system (Wilmington, USA). Electrochemical experiments were performed in a conventional three-electrode cell at 25 °C with a platinum counter electrode and silver-silver chloride (Ag|AgCl|Cl$^-$) electrode as reference electrode. Solutions were prepared with double distilled water and deaerated by bubbling ultra pure nitrogen gas for 30 minutes before use and continued during tests. Working electrode was first immersed into the test solution for 30 min to establish a steady state open circuit potential. EIS measurements were performed at corrosion potentials (E_{corr}) over a frequency range of 0.05–10^5 Hz with a signal amplitude perturbation of 5 mV. Potentiodynamic polarization studies were performed with a scan rate of 0.5 mV/s in the potential range from -400 to $+400$ mV relative to the corrosion potential. Experiments were always repeated at least three times.

2.3. Quantum chemical calculations

Theoretical calculations were carried out at the restricted Hartree–Fock Level (RHF) using MNDO, semi-empirical SCF-MO methods in the HyperChem Release 8.0 packet program implemented on Intel Core 2 Duo computer using relative permittivity 78.4 corresponding to water.

2.4. SEM analysis

Surface analysis were carried out using JEOL-JSM 5600LV SEM. SEM images were obtained from mild steel surface after specimen immersion in 0.1 M HCl solutions in the absence and in the presence of 1×10^{-4} M Schiff bases for 24 h at room temperature.

3. Results and discussion

3.1. Potentiodynamic polarization results

The kinetics of the anodic and cathodic corrosion reactions occurring on mild steel electrodes in 0.1 M HCl solutions with different concentrations of P1, P2 and P3 were studied through the potentiodynamic polarization measurements. All of the obtained potentiodynamic polarization curves are shown in Fig. 2. Electrochemical corrosion parameters such as corrosion potential (E_{corr}), corrosion current density (i_{corr}), cathodic and anodic Tafel slopes (β_c, β_a) obtained from polarization curves by Tafel extrapolation method and the corresponding inhibition efficiency (η) values at different inhibitor concentrations are given in Table 1. The inhibition efficiency at different inhibitor concentrations was calculated from the equation;

$$\eta\% = [1 - (i_{corr^*}/i_{corr})] \times 100 \qquad (1)$$

where i_{corr^*} and i_{corr} are the corrosion current densities for mild steel in the presence and in the absence of inhibitor, respectively.

It is observed from Fig. 2a that both cathodic and anodic curves show a lower current density in the presence of P1 additive than that recorded in HCl solution alone. This suggests that P1 is a mixed type (cathodic/anodic) inhibitor. On the other hand, it can be seen from Fig. 2b and c that the cathodic curves show a lower current density in the presence of the P2 and P3 additives than that recorded in HCl solution. E_{corr} values (Table 1) in the presence of P2 and P3 are shifted to negative direction; this effect is more evident at higher concentrations. These results indicate that P2 and P3 behave as mainly cathodic inhibitors (Yurt et al., 2007; Prabhu et al., 2008).

The inhibition efficiency values in Table 1 show that all the investigated Schiff bases act as effective corrosion inhibitors for mild steel in HCl and their capacity of inhibition increased with increase of concentration. The increase in inhibition efficiency observed at higher inhibitor concentration indicates that more inhibitor molecules are adsorbed on the metal surface thus providing wider surface coverage and these compounds are acting as adsorption inhibitor. These facts suggest that inhibition actions are due to adsorption on steel surface where the adsorbed molecules mechanically screen the coated part of the metal surface from the action of the corrodent.

Examination of experimental data shows that the inhibition efficiency values of the investigated Schiff bases follow the order P1 > P3 > P2. Substitution of bromine and chlorine atom on benzene ring of Schiff bases decreases the inhibition efficiency of compounds P3 and P2 in comparison with unsubstituted P1. The difference in protection actions of the studied inhibitors can be attributed to the presence of the electron-donating group such as Br or Cl. These results show that the presence Cl and Br atoms on the benzene ring in P2 and P3 should decrease the charge density on imine (C=N) group, oxygen and also benzene ring, which are responsible for adsorption. This idea will be discussed in Section 3.5 by using the quantum chemically calculated charge density values of atoms, which act as adsorption centres.

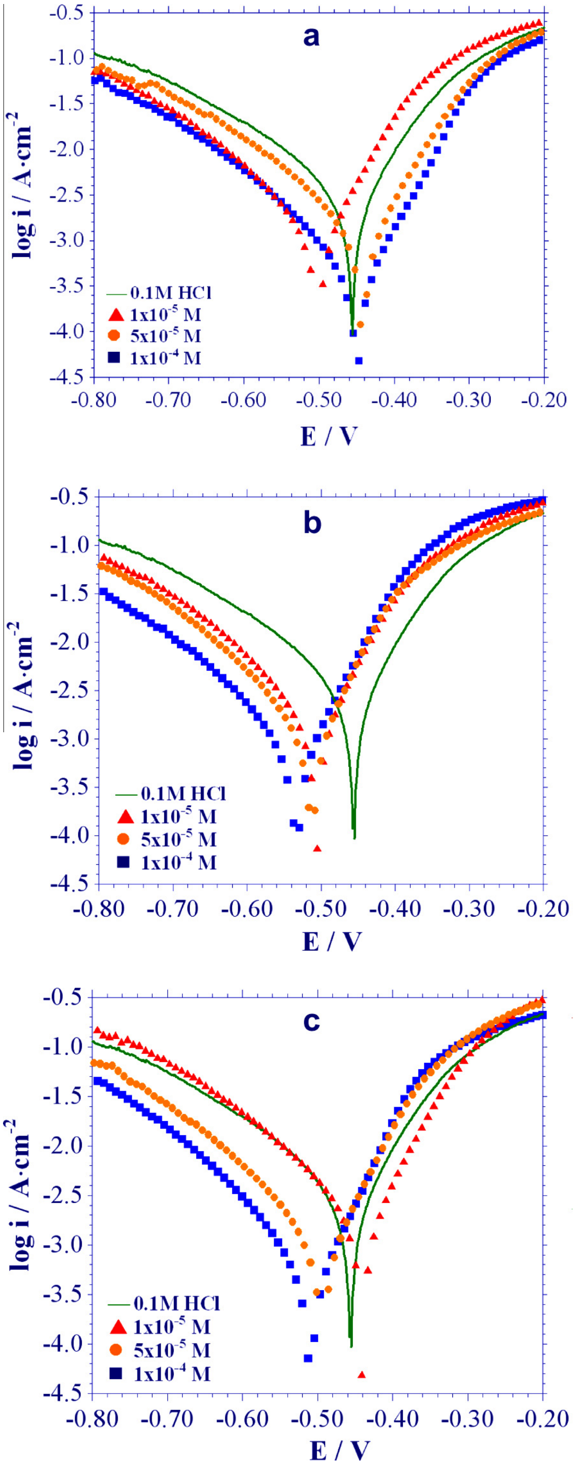

Figure 2 Polarization curves for mild steel in 0.1 M HCl in the presence of various concentrations of (a) P1, (b) P2 and (c) P3.

Table 1 Polarization parameters and the corresponding inhibition efficiencies for mild steel in 0.1 M HCl containing different concentrations of studied Schiff bases at 25 °C.

Inhibitor	C (mol L^{-1})	E_{corr} (mV)	i_{corr} (μA cm^{-2})	β_a (mV dec^{-1})	β_c (mV dec^{-1})	η%	θ
–	–	−442	719.90	98.00	−209.00	–	–
P1	1×10^{-4}	−440	75.35	70.59	−130.00	89.53	0.8953
	7×10^{-5}	−455	143.70	64.00	−130.10	80.03	0.8003
	5×10^{-5}	−436	210.82	77.14	−142.14	70.72	0.7072
	3×10^{-5}	−458	223.27	70.30	−140.50	68.99	0.6889
	1×10^{-5}	−494	281.84	70.27	−163.16	60.85	0.6085
P2	1×10^{-4}	−520	135.94	66.67	−140.91	81.12	0.8112
	7×10^{-5}	−517	196.05	75.43	−125.50	72.27	0.7277
	5×10^{-5}	−508	211.63	72.29	−135.00	70.60	0.7060
	3×10^{-5}	−508	256.23	71.71	−139.43	64.41	0.6441
	1×10^{-5}	−502	348.58	69.77	−150.00	51.58	0.5158
P3	1×10^{-4}	−497	105.50	68.62	−139.13	85.34	0.8534
	7×10^{-5}	−497	146.89	62.86	−138.00	79.59	0.7959
	5×10^{-5}	−481	203.24	69.23	−145.00	71.77	0.7177
	3×10^{-5}	−480	251.19	70.59	−157.11	65.11	0.6511
	1×10^{-5}	−439	309.12	73.14	−158.97	57.06	0.5706

3.2. Electrochemical impedance measurements

Nyquist plots of mild steel in 0.1 M HCl solutions in the presence and in the absence of various concentrations of P1, P2 and P3 are given in Fig. 3. Obtained impedance diagrams have appearance of one capacitive contribution represented by one semi-circle for all solutions examined. Capacitive loop was attributed to charge transfer of the corrosion process and to the formation of a protective layer (Abd El-Rehim et al, 2001). The slightly depressed nature of the semi-circle which has the centre below the x-axis is the characteristic for solid electrodes and such frequency dispersion has been attributed to roughness and other inhomogeneities of the solid electrode (Paskossy, 1994; Jüttner, 1990). A characteristic feature of the results was the absence of a diffusive contribution to real impedance (Z') at low frequencies. This result indicates that adsorbed molecules inhibited anodic dissolution of metal effectively and the corrosion behaviour controlled by charge transfer (Quan et al., 2001).

Nyquist diagrams were modelled by equivalent circuits using ZSimpWin 3.21 software. The proposed equivalent circuit used to fit the experimental results for mild steel is depicted in Fig. 4. In the circuit R_s represents the solution resistance, R_t represents the charge transfer resistance and Q represents a constant phase element (CPE). This is similar to Randles cell but with a constant phase element (CPE) or a CPE with diffusion instead of double layer capacitance. CPE elements are used to account for deviations brought by surface roughness because the impedance of double layer does not behave as an ideal capacitor in the presence of dispersing effect (Emregül and Atakol, 2003; McCafferty, 1997). The impedance of constant phase element Z_{CPE} is defined by two values, Y_o and n. The factor n, defined as CPE power, can serve as a measure of the surface heterogeneity (Lopez et al., 2003). In corrosion studies, the low value of n can be attributed to the roughening of the electrode surface. The impedance Z_{CPE} can be calculated with the Eq. (2):

$$Z_{\mathrm{CPE}} = Y_o^{-1}(j\omega)^{-n} \tag{2}$$

The results of correlation of experimental data with equivalent circuit (Fig. 4) and the calculated impedance parameters of all examined inhibitors are given in Table 2. Percent inhibition efficiencies (% η) were calculated using the following formula (Eq. (3)).

$$\eta\% = [1 - (R_t/R_{t^*})] \times 100 \tag{3}$$

where R_{t^*} and R_t are values of the charge transfer resistance with and without inhibitor, respectively.

As can be seen from Table 2 and Fig. 3, the R_t values of all the investigated Schiff bases increase with increasing inhibitor concentration. This is due to increasing surface coverage by inhibitors which leads to an increase in η values with increasing inhibitor concentration.

3.3. Adsorption mechanism

As can be seen from Tables 1 and 2 all the examined Schiff bases are effective corrosion inhibitors for acidic corrosion of mild steel and their inhibition efficiency values increased as their concentrations are increased. These facts can be explained by the adsorption of these compounds on mild steel surface. The adsorption process of inhibitors is influenced by the chemical structures of organic compounds, the nature and surface charge of metal, the distribution of charge in molecule and the type of aggressive media (Saleh and Shams El Din, 1972; Maayta and Al-Rawashdeh, 2004).

Since adsorption isotherms can provide important clues to the nature of metal-inhibitor interaction, it was established that isotherms describe the adsorption behaviour of the studied corrosion inhibitor. Determination of the type of adsorption isotherm is achieved by taking into account the degree of surface coverage, θ, as a function of inhibitor concentration. The surface coverage values were calculated from Eq. (4):

$$\theta = [1 - (i_{corr^*}/i_{corr})] = [1 - (R_t/R_{t^*})] \tag{4}$$

Several adsorption isotherms were assessed and the Temkin adsorption isotherm was found to provide the best description of the adsorption behaviour of the investigated Schiff bases,

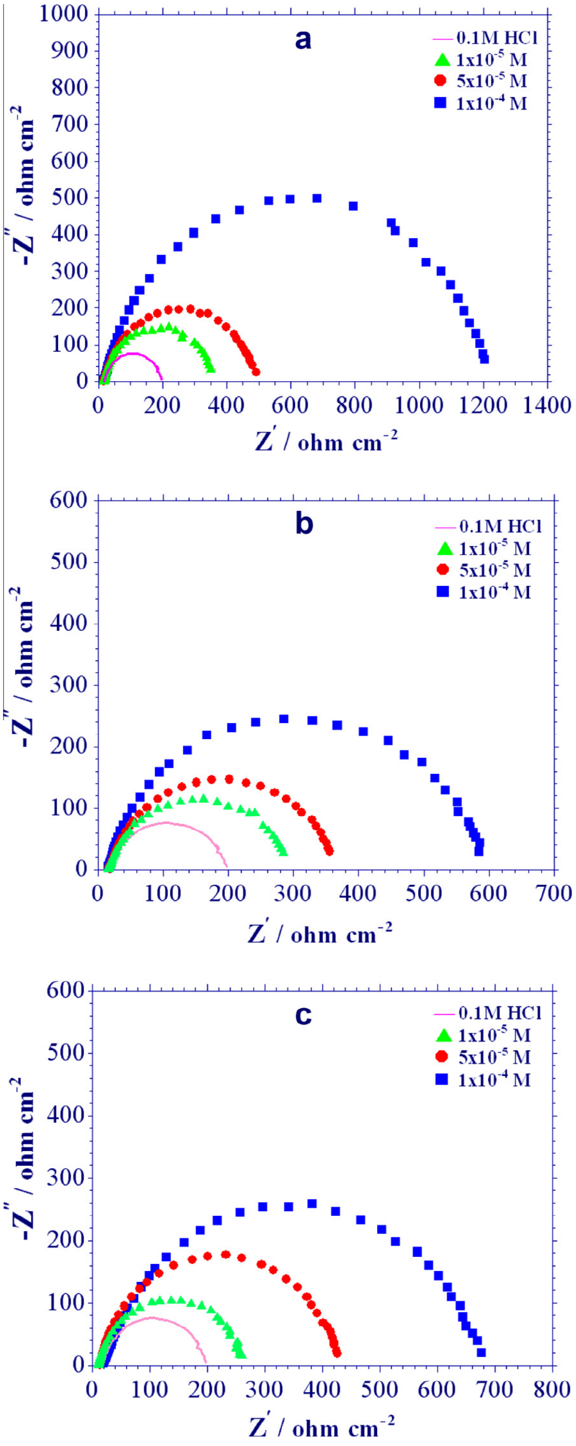

Figure 3 Impedance plots of mild steel obtained in 0.1 M HCl in the presence of various concentrations of (a) P1, (b) P2 and (c) P3.

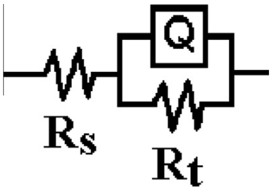

Figure 4 Electrochemical equivalent circuit diagram for metal–electrolyte interface.

which has the following surface coverage, θ, and the bulk concentration, c, relationship (Hosseini et al., 2003);

$$e^{f\theta} = K_{\mathrm{ads}}c \tag{5}$$

where K_{ads} is the adsorption equilibrium constant and f is the molecular interaction constant.

Typical plots of θ versus ln c for P1, P2 and P3 are given in Fig. 5. From the obtained straight lines in θ –ln c graphs, equilibrium constants for adsorption process, K_{ads}, were obtained. The equilibrium constants for adsorption process are related to the free energy of adsorption, ΔG_{ads}, by,

$$\Delta G_{\mathrm{ads}} = -RT\ln(55.5\,K_{\mathrm{ads}}) \tag{6}$$

where 55.5 is the molar concentration of water in the solution. The thermodynamic parameters for adsorption process obtained from Temkin adsorption isotherms for the studied molecules are given in Table 3. The values of free energy of adsorption, ΔG_{ads}, are negative which reveals the spontaneity of adsorption process and the stability of the adsorbed layer on the steel surface. The obtained values of the adsorption free energy, ΔG_{ads}, −48 to −51 kJ/mol are indicative of chemisorption (Szlarska-Smialowska, 1978).

In order to predict the corrosion inhibition mechanism of Schiff bases via adsorption, corrosion mechanism of metal must be known. The following mechanism is proposed for the corrosion of iron and steel in hydrochloric acid (Morad et al., 1995; Aramaki et al., 1987). According to this mechanism anodic dissolution of iron follows the steps:

$$\mathrm{Fe} + \mathrm{Cl}^- \rightleftharpoons (\mathrm{FeCl}^-)_{\mathrm{ads}} \tag{i}$$

$$(\mathrm{FeCl}^-)_{\mathrm{ads}} \rightleftharpoons (\mathrm{FeCl})_{\mathrm{ads}} + \mathrm{e}^- \tag{ii}$$

$$(\mathrm{FeCl})_{\mathrm{ads}} \rightleftharpoons \mathrm{FeCl}^+ + \mathrm{e}^- \tag{iii}$$

$$\mathrm{FeCl}^+ \rightleftharpoons \mathrm{Fe}^{2+} + \mathrm{Cl}^- \tag{iv}$$

The cathodic hydrogen evolution follows the steps:

$$\mathrm{Fe} + \mathrm{H}^+ \rightleftharpoons (\mathrm{FeH}^+)_{\mathrm{ads}} \tag{v}$$

$$(\mathrm{FeH}^+)_{\mathrm{ads}} + \mathrm{e}^- \rightarrow (\mathrm{FeH})_{\mathrm{ads}} \tag{vi}$$

$$(\mathrm{FeH})_{\mathrm{ads}} + \mathrm{H}^+ + \mathrm{e}^- \rightarrow \mathrm{Fe} + \mathrm{H}_2 \tag{vii}$$

All of these steps indicate that the corrosion rate of iron and steel in hydrochloric acid is controlled by both hydrogen evolution reaction and dissolution reaction of iron.

In acidic media Schiff base molecules exist in the form of protonated species (Asshassi-Sorkhabi et al., 2006). Inhibitor performance of protonated Schiff base molecules can be explained by three different adsorption mechanisms (Fig. 6) (Ahamad, 2010b):

(1) Adsorption can occur via electrostatic interaction between a negatively charged surface, which is provided with a specifically adsorbed anion on metal surface ($(\mathrm{FeCl}^-)_{\mathrm{ads}}$ species), and the positive charge of the inhibitor. Protonated form with positively charged part of the molecule is oriented toward negatively charged surface (Keles et al., 2008). (*physical adsorption*)

Table 2 Impedance parameters and the corresponding inhibition efficiency values for mild steel in 0.1 M HCl containing different concentrations of studied Schiff bases at 25 °C.

Inhibitor	C (mol L^{-1})	R_s (Ω cm^{-2})	Q (Ss^{-n} cm^{-2})	n	R_t (Ω cm^{-2})	E_{corr} (mV)	η%	θ
–	–	17.82	4.23×10^{-5}	0.87	182.2	−465	–	–
P1	1×10^{-4}	18.81	1.83×10^{-5}	0.86	1226	−455	85.14	0.8514
	7×10^{-5}	17.51	2.71×10^{-5}	0.84	493.3	−453	63.07	0.6307
	5×10^{-5}	14.47	2.61×10^{-5}	0.90	464.6	−522	60.78	0.6078
	3×10^{-5}	10.92	5.13×10^{-5}	0.90	360.2	−474	49.42	0.4942
	1×10^{-5}	17.54	8.11×10^{-5}	0.87	348.9	−520	47.78	0.4778
P2	1×10^{-4}	16.38	3.86×10^{-5}	0.89	579.4	−521	68.55	0.6855
	7×10^{-5}	15.31	5.44×10^{-5}	0.87	405.9	−533	55.11	0.5511
	5×10^{-5}	17.86	6.82×10^{-5}	0.87	352.2	−525	48.27	0.4827
	3×10^{-5}	20.18	8.05×10^{-5}	0.84	324.2	−527	43.80	0.4380
	1×10^{-5}	16.25	9.08×10^{-5}	0.84	284.6	−522	35.98	0.3598
P3	1×10^{-4}	18.22	2.05×10^{-5}	0.80	687.6	−539	73.50	0.7350
	7×10^{-5}	16.22	2.16×10^{-5}	0.89	519.8	−521	64.95	0.6495
	5×10^{-5}	13.50	2.48×10^{-5}	0.89	416.2	−502	56.22	0.5622
	3×10^{-5}	14.85	3.28×10^{-5}	0.89	326.9	−505	44.26	0.4426
	1×10^{-5}	10.83	4.79×10^{-5}	0.87	274.2	−450	33.56	0.3356

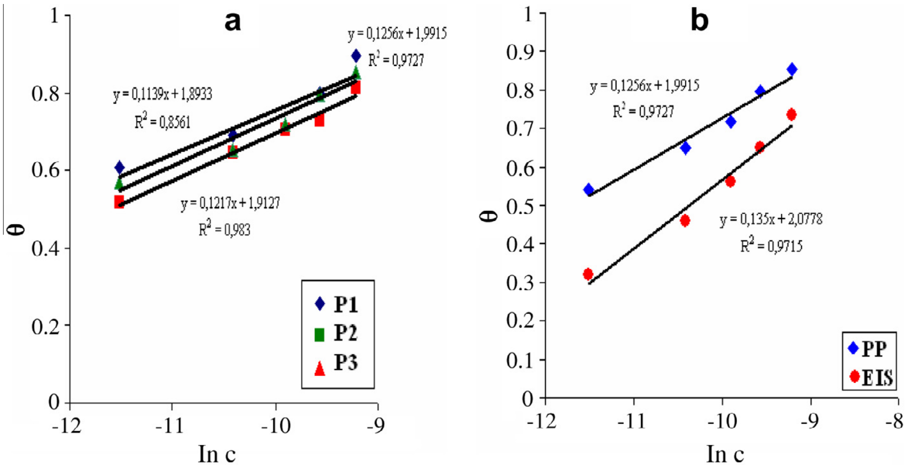

Figure 5 (a) Temkin adsorption isotherms of P1, P2 and P3 obtained by using surface coverage values calculated by the potentiodynamic polarization results, (b) plot of Temkin adsorption isotherm of P3 obtained by the potentiodynamic polarization (PP) and EIS results.

Table 3 Thermodynamic parameters of adsorption obtained by potentiodynamic polarization measurements for studied Schiff bases on mild steel in 0.1 M HCl solutions at 25 °C.

Inhibitor	K_{ads} (dm^{-3} mol^{-1})	ΔG_{ads} (J mol^{-1})	f
P1	16.60×10^6	−51141	8.780
P2	6.67×10^6	−48882	8.210
P3	7.71×10^6	−49239	7.962

(2) The protonated molecules can adsorb on the cathodic sites of steel in competition with the hydrogen ions (step v). Therefore the activation polarization of cathodic reaction increases. (*physical adsorption*)

(3) Chemisorption of Schiff bases due to interaction of their π orbitals and/or interaction of unshared electron pairs on N and O atoms with the metal surface may occur following the deprotonation step of the physically adsorbed protonated forms of Schiff bases (Fig. 6b). (*chemical adsorption*)

(4) The existing data show that all of the investigated Schiff bases act as inhibitor by chemisorption onto the metal surface. P1 suppresses both the anodic metal dissolution reaction and the cathodic hydrogen evolution reaction (adsorption mechanism 1–3), while P2 and P3 are effective inhibitors on just the cathodic corrosion reaction (adsorption mechanism 2 and 3). These results show that inhibitor performance and also inhibition mechanism are affected by molecular structure. Substitutions of the electron-donating group such as Br or Cl in the benzene ring of inhibitors prevent the adsorption of the molecules onto the anodic sites of the metal surface. The presence of Cl and Br atoms on the benzene ring in P2 and P3 decreases the charge densities on N and O atoms, which are responsible for adsorption. In addition, the presence of Cl and Br as additional negatively charged atoms in the molecular structures of P2 and P3 minimizes the probability

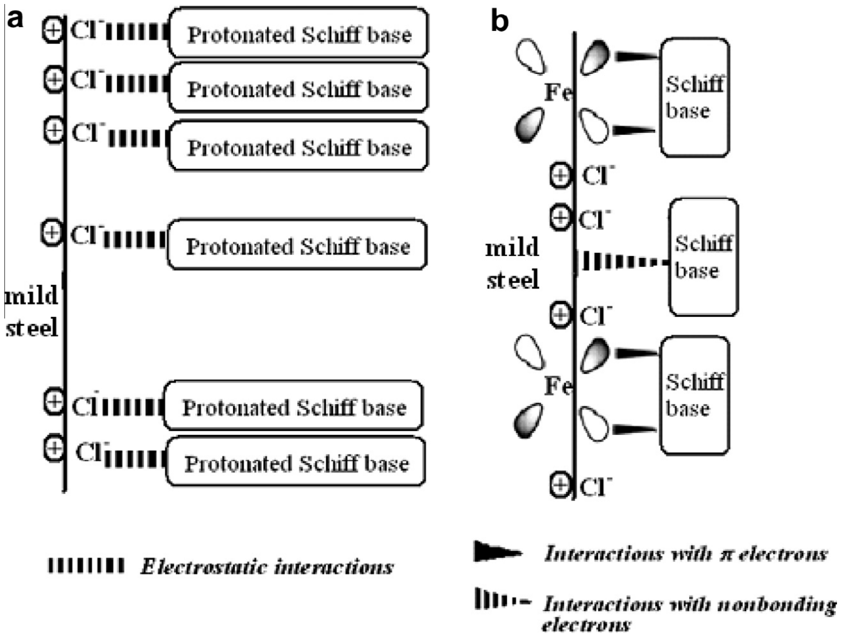

Figure 6 Schematic illustration of different adsorption modes of Schiff bases on mild steel.

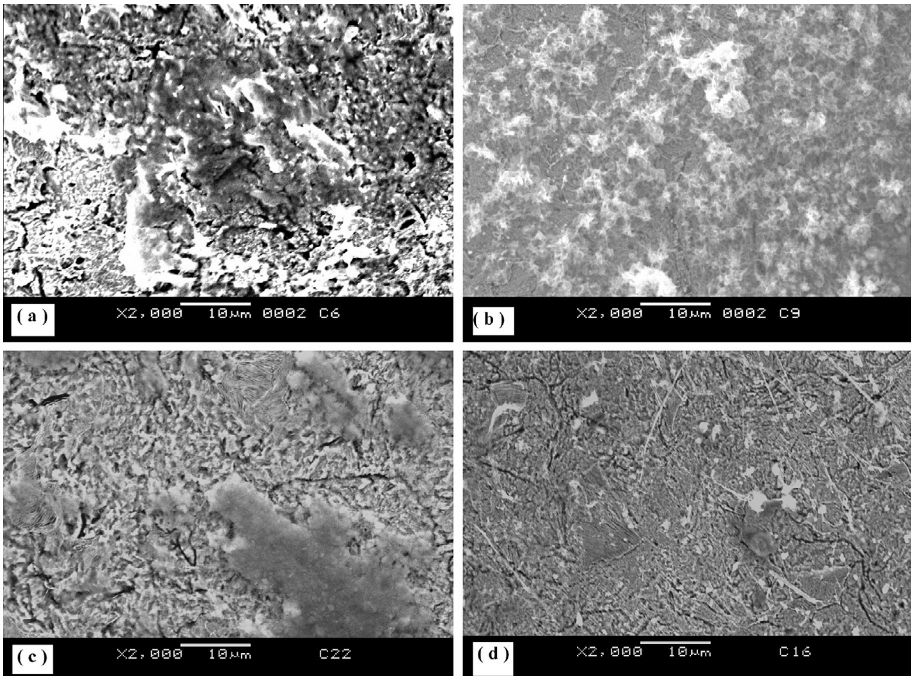

Figure 7 SEM images of mild steel after immersion in 0.1 M HCl for 24 h (a) in the absence of inhibitor and in the presence of 1×10^{-4} M (b) P1, (c) P2 and (d) P3.

of electrostatic interaction between Schiff bases and $(FeCl^{-})_{ads}$ species (step i) on the anodic sites of metal.

3.4. SEM observations

The scanning electron micrographs (SEM) were taken and observed in order to support our findings. Fig. 7a–d shows the scanning electron micrographs for mild steel after immersion for 24 h in 0.1 M HCl solution without and with P1, P2 and P3. The specimen surface in Fig. 7a appears to be roughened extensively by the corrosive environment and the porous layer of corrosion product is present. Examination of Fig. 7b–d reveals that the specimens immersed in the inhibitor solutions are in better conditions having smooth surfaces compared with that of the surface immersed in 0.1 M HCl alone.

This indicates that the compounds hinder the dissolution of iron and thereby reduce the rate of corrosion.

3.5. Quantum chemical calculations

Experimental results show that inhibition efficiencies of the studied Schiff bases can be due to the chemical adsorption of inhibitor molecules onto metal surface. Chemisorption involves the share or transfer of charge from the molecules to the surface to form a coordinate type bond. Electron transfer is typical for transition metals having vacant low-energy orbitals. As for inhibitors, the electron transfer can be expected with compounds having relatively loosely bound electrons (Mansfeld, 1987; Yurt et al., 2005a,b). In our case, coordinate covalent bond formation between electron pairs of unprotonated N and O atoms in molecules and metal surface can take place. In addition, chemisorption of Schiff bases due to interaction of their π electrons with metal surface occurs following deprotonation step of the physically adsorbed protonated forms of Schiff bases.

To investigate the effect of molecular structure on the inhibition mechanism and the inhibition efficiency, some quantum chemical calculations were performed. Quantum chemical parameters such as the energy of the highest occupied molecular orbital, E_H, the energy of the lowest unoccupied molecular orbital, E_L, the differences between them ($E_L - E_H$), HOMO–LUMO gap, dipole moment, μ, of molecules and the charge densities on the Cl, Br, O and N atoms as adsorption centres in molecules of Schiff bases have been obtained from MNDO semi-empirical method and are given in Table 4.

As can be seen from Table 4, there was no direct relationship between the η and charges of oxygen, q_O, nitrogen, q_N and the dipole moment of molecule, μ. However, the inhibition efficiencies of these Schiff bases increase when E_H increase, $E_L - E_H$ values decrease. If a first-order linear regression analysis was made of relationship between η and E_H or $E_L - E_H$ values of the investigated Schiff bases, the following equations were obtained:

$$\eta = 2.649 + 0.2041E_H \ (r = 0.986) \quad (7)$$

$$\eta = 3.079 - 3.4756E_L - E_H \ (r = 0.910) \quad (8)$$

Table 4 Calculated quantum chemical parameters of studies Schiff bases.

Inhibitor	P1	P2	P3
η%	89.53	81.12	85.34
E_H (eV)	−8.612	−9.018	−8.772
E_L (eV)	−0.216	−0.604	−0.359
$E_L - E_H$ (eV)	8.396	8.418	8.413
μ (Debye)	5.021	4.270	8.937
$q_{N(1)}$	−0.210	−0.202	−0.208
$q_{N(2)}$	−0.278	−0.255	−0.268
$q_{O(1)}$	−0.291	−0.291	−0.285
$q_{O(2)}$	−0.254	−0.245	−0.245
$q_{O(3)}$	−0.300	−0.299	−0.291
$q_{O(4)}$	−0.242	−0.240	−0.241
$q_{Br(1)}$	–	–	−0.039
$q_{Br(2)}$	–	–	−0.039
$q_{Cl(1)}$	–	−0.111	–
$q_{Cl(2)}$	–	−0.114	–

The obtained equations and Table 4 show that an increase in the values of E_H and a decrease in $E_L - E_H$ values cause increase in the inhibitive action of the studied Schiff bases. It is known that in the chemical adsorption an increase in E_H values causes a significant increase in the inhibition efficiency of organic compounds (Li et al., 1999a,b). On the other hand, the energy gap between E_L and E_H can be used as a characteristic quantity for metallic complexes (Cherry et al., 1977; Yurt et al., 2005a,b). The lower energy gap indicates the higher stability of the formed complex, thus the higher inhibition efficiency. Increase in η values with the decrease of $E_L - E_H$ values indicates the formation of coordinate covalent bond between organic molecules and mild steel. So, the positive sign of the coefficient of E_H and the negative sign of the coefficient of $E_L - E_H$ suggest that these Schiff bases are adsorbed on steel surface by chemical mechanism.

The variation in the inhibition efficiency of P1, P2 and P3 depends on the presence of electronegative Cl and Br atoms as substituent in the molecular structure of P2 and P3, respectively. Table 4 shows that the presence of Cl and Br atoms on the benzene ring in P2 and P3 decreases the charge densities ($q\mathrm{N}_1$ and $q\mathrm{N}_2$) on N atoms in imine groups that are responsible for adsorption. In addition, the presence of Cl and Br as additional negatively charged atoms in the molecular structures of P2 and P3 minimizes the probability of electrostatic interaction between protonated forms of Schiff bases and $(\mathrm{FeCl}^-)_{ads}$ species (step i) on the anodic sites of metal. Therefore, P2 and P3 are mainly effective on cathodic reaction and the inhibition of corrosion of mild steel in 0.1 M HCl solution by P2 and P3 is predominantly under cathodic control. On the other hand, interactions between P1 and both the cathodic and anodic sites of steel surfaces can occur. So, P1 acts as a mixed type inhibitor.

4. Conclusions

- All studied Schiff bases behave as efficient corrosion inhibitors and their inhibition efficiencies tend to increase with increasing inhibitor concentration.
- The protection ability of these compounds is given in the order of P1 > P3 > P2.
- P1 acts as a mixed type inhibitor while P2 and P3 behave as cathodic inhibitors for acidic corrosion of steel.
- The inhibition action of the studied compounds is mainly due to their adsorption on the mild steel surface. Adsorption process obeys Temkin adsorption isotherm.
- The thermodynamic parameters (K_{ads}, ΔG_{ads}) of adsorption for the studied compounds are calculated from their adsorption isotherms. The negative values of $\Delta\Delta G_{ads}$ show the spontaneity of the adsorption.
- The inhibition efficiencies of the studied Schiff bases increase when E_H increases, $E_L - E_H$ values decrease.
- The values of free energy of adsorption and the relationship between the inhibition efficiency values and the calculated quantum chemical parameters suggest that these Schiff bases can be adsorbed on mild steel surface by chemical mechanism.

Acknowledgement

This work was supported by the Commission of Scientific Research Projects of Eskisehir Osmangazi University

(ESOGU/200719038). The authors gratefully acknowledge the financial support by Eskişehir Osmangazi University.

References

Abd El-Rehim, S.S., Hassan, H.H., Amin, M.A., 2001. Mater. Chem. Phys. 70, 64–72.

Ahamad, I., Prasad, R., Quraishi, M.A., 2010a. Corros. Sci. 52, 933–942.

Ahamad, I., Prasad, R., Quraishi, M.A., 2010b. Corros. Sci. 52, 1472–1481.

Aramaki, K., Hagiwara, N., Nishihara, H., 1987. Corros. Sci. 27, 487–497.

Asshassi-Sorkhabi, H., Shabani, B., Aligholipour, B., Seifzadeh, D., 2006. Appl. Surf. Sci. 252, 4039–4047.

Bahrami, M.J., Hosseini, S.M.A., Pilvar, P., 2010. Corros. Sci. 52, 2793–2803.

Bain, C.D., Troughton, E.B., Tao, Y.T., Evall, J., Whitesides, G.M., Nuzzo, R.G., 1989. J. Am. Soc. 111, 321–335.

Bentiss, F., Lagrenee, M., Elmehdi, B., Mernari, B., Traisnel, M., Vezin, H., 2002. Corrosion 58, 399–407.

Cherry, W., Epiotis, N., Borden, W.T., 1977. Acc. Chem. Res. 10, 167–173.

Clubby, B.G., Chemical Inhibitors for Corrosion Control, Royal Soc. Chem., Cambridge, pp. 141–148.

Emregül, K.C., Kurtaran, R., Atakol, O., 2003. Corros. Sci. 45, 2803–2817.

Emregül, K.C., Atakol, O., 2003. Mater. Chem. Phys. 82, 188–193.

Fouda, A.S., Ellithy, A.S., 2009. Corros. Sci. 51, 868–875.

Gomma, G.K., Wahdan, M.H., 1995. Mater. Chem. Phys. 39, 209–213.

Hosseini, M., Mertens, S.F.L., Ghorbani, M., Arshadi, M.R., 2003. Mater. Chem. Phys. 78, 800–808.

Ju, H., Kai, Z., Li, Y., 2008. Corros. Sci. 50, 865–871.

Jüttner, K., 1990. Electrochim. Acta 35, 1501–1508.

Keles, H., Keles, M., Dehri, I., Serindag, O., 2008. Mater. Chem. Phys. 112, 173–179.

Li, S., Chen, S., Lei, S., Ma, H., Yu, R., Liu, D., 1999a. Corros. Sci. 41, 1273–1287.

Li, S.L., Wang, Y.G., Chen, S.H., Yu, R., Lei, S.B., Ma, H.Y., Liu, D.X., 1999b. Corros. Sci. 41, 1769–1782.

Lopez, D.A., Simison, S.N., de Sanchez, S.R., 2003. Electrochim. Acta 48, 845–854.

Nathan, C.C., 1977. Organic Inhibitors. NACE, Houston, TX, pp. 11–17.

Negm Nabel, A., Zaki Mohamed, F., 2008. Colloids Surf. A: Physicochem. Eng. Aspects 322, 97–102.

Maayta, A.K., Al-Rawashdeh, M.A.F., 2004. Corros. Sci. 46, 1129–1140.

Mansfeld, F., 1987. Corrosion Mechanisms. Marcel Dekker, New York, pp. 119–121..

McCafferty, E., 1997. Corros. Sci. 39, 243–254.

Morad, M., Morvan, J., Pagetti, J., 1995. In: Proceedings of the 8th European Symposium on Corrosion Inhibitors (8SEIC), Sez. V (Suppl. 10). Ann. Univ. Ferrara, NS, pp. 159–167.

Moretti, G., Quartarone, G., Tassan, A., Zlngales, A., 1996. Electrochim. Acta 41, 1971–1980.

Özcan, M., Dehri, İ., Erbil, M., 2004. Appl. Surf. Sci. 236, 155–164.

Paskossy, T., 1994. J. Electroanal. Chem. 364, 111–125.

Prabhu, R.A., Venkatesha, T.V., Shanbag, A.V., Kulkarni, G.M., Kalkhambkar, R.G., 2008. Corros. Sci. 50, 3356–3362.

Quan, Z., Wu, X., Chen, S., Zhao, S., Ma, H., 2001. Corrosion 57, 195–201.

Saleh, R.M., Shams El Din, A.M., 1972. Corros. Sci. 12, 689–697.

Shokry, H., Yuasa, M., Sekine, I., Issa, R.M., El-Baradie, H.Y., Gomma, G.K., 1998. Corros. Sci. 40, 2173–2186.

Stupnisek-Lisac, E., Ademovic, Z., 1995. In: Proceeding of the Eighth European Symposium on Corrosion Inhibitors (8SEIC), Sez. V (Suppl.). Ann. Univ. Ferrara, NS, pp. 257–265.

Szlarska-Smialowska, Z., 1978. Corros. Sci. 18, 97–101.

Trabanelli, G., 1991. Corrosion 47, 410–419.

Yurt, A., Balaban, A., Kandemir, S.Ü., Bereket, G., Erk, B., 2004. Mater. Chem. Phys. 85, 420–426.

Yurt, A., Bereket, G., Kıvrak, A., Balaban, A., Erk, B., 2005a. J. Appl. Electrochem. 35, 1025–1032.

Yurt, A., Bereket, G., Öğretir, C., 2005b. J. Mol. Struct. THEOCHEM 725, 215–221.

Yurt, A., Ulutaş, Ş., Dal, H., 2006. Appl. Surf. Sci. 253, 919–925.

Yurt, A., Bütün, V., Duran, B., 2007. Mater. Chem. Phys. 105, 114–121.